

## Original Article

# MicroRNA-130a regulates cell malignancy by targeting RECK in chronic myeloid leukemia

Quan Li<sup>1\*</sup>, Yaohui Wu<sup>2\*</sup>, Jian Zhang<sup>1</sup>, Tienan Yi<sup>1</sup>, Weiming Li<sup>2</sup>

<sup>1</sup>Department of Oncology, Xiangyang Central Hospital, Hubei University of Arts and Science, Xiangyang 441021, China; <sup>2</sup>Department of Hematology, Union Hospital, Tongji Medical College, Huazhong University of Science and Technology, 1277# Jiefang Avenue, Wuhan 430022, China. \*Equal contributors.

Received February 13, 2015; Accepted January 26, 2016; Epub February 15, 2016; Published February 29, 2016

**Abstract:** Emerging evidence has indicated that microRNAs are involved in tumor development and progression, acting as either tumor suppressors or oncogenes. In this study, we aimed to investigate the role of miR-130a in the pathogenesis of chronic myeloid leukemia (CML). Functional studies indicate that over-expression of miR-130a in A562 CML cells dramatically suppresses cell proliferation and induces cell apoptosis both *in vitro* and *in vivo*. Furthermore, we demonstrate that the transcriptional regulator RECK is a target of miR-130a. In conclusion, our study suggests that miR-130a may function as a novel tumor suppressor in CML, and its anti-oncogenic activity may involve the direct targeting and inhibition of RECK.

**Keywords:** Chronic myeloid leukemia (CML), A562, miR-130a, RECK, invasion, migration, target therapy

## Introduction

Chronic myeloid leukemia (CML) is a myeloproliferative disease originating from a constitutively active tyrosine kinase, BCR-ABL [1]. Understanding the molecular pathogenesis of CML may enable advancements in the diagnosis and treatment of this disease. CML progression depends on the capacity to invade and to metastasize to distant sites. Tumor cell metastasis is thought to be controlled by molecular processes that are different from those that control tumor initiation and growth [2]. Support for this hypothesis comes from the observation of human cancer lesions as well as several mouse models in which tissue-specific oncogene expression led to tumor initiation, yet tumor progression was not observed [3-5]. The metastatic process is complex because it involves several distinct steps such as tumor cell dispersal from the epithelium, invasiveness, intravasation into lymph or blood vessels, dissemination, and extravasation into a remote organ and colonization of this organ [6].

MicroRNAs (miRNAs) are short, endogenous non-coding RNAs that silence protein expression by interacting with the 3'-UTRs of their target gene mRNAs. Recent studies have demon-

strated that miRNAs can function as tumor suppressors or oncogenes in various cancers [7]. It has been confirmed that the development and progression of gastric cancer may be attributed to miRNAs [8]. In our previous work, we found numerous putative miRNAs of differential expression by comparing the miRNA expression profile in 28 CML cancer stem cells and their corresponding normal MSCs [9, 10]. In addition to the well-known miRNAs, such as miR-375, miR-29c, miR-31, miR-199-3p, miR-409-3p [11] and the miR-200 family, we found that miR-130a was rarely researched and was one of the most significantly down-regulated miRNAs in CML.

RECK (reversion-inducing cysteine-rich protein with Kazal motifs), a tumor oncogene, promotes some of the MMPs involved in the breakdown of the extracellular matrix (ECM) and angiogenesis. These MMPs include MMP-2, MMP-9 and MMP-13, all of which are known to be involved in cancer progression [12]. Thus, it has a significant effect on carcinogenesis by promoting angiogenesis and invasion of tumors through the ECM. RECK expression is frequently reduced in several common cancers, and the level of residual RECK expression in cancer tissues correlates with better prognosis [13]. Studies on

## Mir-130a targets RECK in CML

RECK gene regulation may therefore yield important insights into the mechanisms of carcinogenesis.

In this study, we explored the possibility that miR-130a may be involved in CML carcinogenesis. Our objectives were to investigate the expression level of miR-130a in CML, to explore its effect on cell proliferation, and to understand its molecular mechanism of function in tumor pathogenesis.

### Materials and methods

#### *Cell culture and transfection*

Human CML cell line A562 was purchased from the American Type Culture Collection and cultured in RPMI 1640 medium containing 10% fetal bovine serum (FBS) with 100 µg/ml penicillin/streptomycin at 37°C with 5% CO<sub>2</sub>. Transfection was performed with Lipofectamine 2000 (Invitrogen, CA, USA) according to the manufacturer's protocol. Total RNA and protein were prepared 48 h after transfection and were used for qRT-PCR or Western blot analysis.

#### *Tissue samples*

CML cancer stem cells were collected from patients with advanced CML at Yinzhou People's Hospital (Ningbo, China) between January 2012 and March 2014. Informed consent was obtained from all subjects and this study was approved by the Clinical Research Ethics Committee of Yinzhou People's Hospital.

#### *MicroRNA real-time PCR*

To collect microRNA,  $1 \times 10^2$ – $1 \times 10^7$  cells were harvested, washed in PBS once, and stored on ice. Complete cell lysate was prepared by adding 600 µl lysis binding buffer, and the samples were vortexed. Then, 60 µl microRNA aomogenete additive was added to the cell lysate and mixed thoroughly by inverting several times. The sample was stored on ice for 10 min, followed by addition of an equal volume (600 µl) of phenol: chloroform (1:1) solution. The sample was mixed by inverting for 30-60 sec and then centrifuged at 12000 g for 5 min. The supernatant was transferred to a new tube, and the volume was estimated. One-third volume of 100% ethanol was added and mixed. The mixture was loaded to the column at room temperature and centrifuged at 10000 g for 15 sec.

The flow-through was collected, and the volume was then estimated. Two-thirds volume of 100% ethanol was added and mixed. The mixture was loaded onto the column at room temperature and centrifuged at 10000 g for 15 sec. The flow-through was discarded and 700 µl of microRNA wash solution was added to the column, followed by centrifugation at 10000 for 10 sec. The flow-through was discarded again, and 500 µl of microRNA wash solution was added to the column, followed by centrifugation at 10000 for 10 sec. The flow-through was discarded a third time, the column was transferred to a new tube, and 100 µl of pre-heated elution solution (95 degree) was added at room temperature. The RNA was then collected by centrifugation at 12000 g for 30 sec.

#### *Western blot*

Cells were harvested, washed twice in PBS, and lysed in lysis buffer (protease inhibitors were added immediately before use) for 30 min on ice. Lysate was centrifuged at 10000 rpm, and the supernatants were collected and stored at -70°C in aliquots. All procedures were carried out on ice. Protein concentration was determined using a BCA assay kit (Tianlai Biotech).

#### *Cell viability assay*

Cells were seeded into 96-well plates ( $2 \times 10^3$  cells/well) directly or 24 hours after transfection and allowed to attach overnight. Freshly prepared cisplatin was then added with different final concentrations. Forty-eight hours later, cell viability was assessed via a 3-(4,5-dimethylthiazol-2-yl)-2,5-diphenyl-tetrazolium bromide (MTT) assay as described previously [13].

#### *Wound-healing assay*

A wound-healing assay was used to assess capacity for tumor cell motility. Briefly, cells ( $1 \times 10^6$ /well) were seeded in six-well plates, cultured overnight, and transfected with miR-130a mimics or inhibitors and the respective controls. On reaching confluency, the cell layer was scratched with a sterile plastic tip and then washed with culture medium twice and cultured again for up to 48 or 72 h with serum-reduced medium containing 1% FBS. Photo images of the plates were taken under a microscope. The gap closure was measured at 48 or 72 h, and the data were summarized based on sextuple assays for each experiment.

## Mir-130a targets RECK in CML

### *Migration and invasion assays*

We used a Transwell insert (24-well insert, pore size 8  $\mu$ m; Corning, Inc., Corning, NY) to determine the effect of miR-625 on CML cell migration and invasion in vitro. Briefly, the transfected cells were first starved in serum-free medium overnight, and  $3 \times 10^4$  cells were resuspended in serum-free medium and placed in the top chambers in triplicate. The lower chamber was filled with 10% FBS as the chemoattractant and incubated for 48 h for the migration assay and 72 h for the invasion assay. For the invasion assay, the inserts were previously coated with extracellular matrix gel (BD Biosciences, Bedford, MA). At the end of each experiment, the cells on the upper surface of the membrane were removed, and the cells on the lower surface were fixed and stained with 0.1% crystal violet. Five visual fields of each insert were randomly chosen and counted under a light microscope.

### *Plasmid construction and luciferase reporter assay*

Wild-type 3'untranslated region (3'UTR) of RECK containing predicted miR-15b target sites were amplified by PCR from A562 cell genomic DNA. Primers used: Forward: GAT CTG CAG GGG TTA GCT TGG GGA CCT GAA C; Reverse: GAT CAT ATG AGA GTG ACA TAC TGA TGC CTA C. Mutant 3'UTRs were generated by overlap-extension PCR method. Both wild-type and mutant 3'UTR fragments were subcloned into the pGL3-control vector (Promega, Madison, WI) immediately downstream of the stop codon of the luciferase gene. DNA fragment coding RECK protein was amplified by PCR from A562 cell cDNA and cloned into pCMV-Myc expression vector (Clontech, Mountain View, CA). Primers used: Forward: GCT GAA TTC ATG CCG GTG GAC CTC AGC AAG T; Reverse: CTG CTC GAG CTA CTT CCC AGA CAG CTG CTC G. For the luciferase assay, the reporter plasmid was co-transfected with a control Renilla luciferase vector into A562 cells in the presence of either miR-130a or NC. After 48 h, the cells were harvested, and the luciferase activity was measured using the Dual-Luciferase Reporter Assay System (Promega, Madison, WI, USA).

### *Animal studies*

Five-week-old female BALB/c nude mice were purchased from the Animal Center of Zhejiang

University (Hangzhou, China). For *in vivo* chemosensitivity and metastasis assays, A562 cells (infected with either the miR-130a-overexpressing lentivirus or the mock lentivirus) were subcutaneously inoculated into nude mice (six per group,  $1 \times 10^6$  cells for each mouse). Tumor growth was examined every other day. Tumor volumes were calculated using the equation  $V = A \times B^2/2$  ( $\text{mm}^3$ ), where A is the largest diameter and B is the perpendicular diameter. When the average tumor size reached  $\approx 50 \text{ mm}^3$ , cisplatin was administered via intraperitoneal injection at a dose of 5 mg/kg, 1 dose every other day, with 3 doses in total. After 2 weeks, all mice were sacrificed. Transplanted tumors were excised, and tumor tissues were used to perform hematoxylin & eosin (H&E) staining. All research involving animals complied with protocols approved by the Zhejiang medical experimental animal care commission.

### *Data analysis*

The results are expressed as the mean  $\pm$  standard deviation. Data were analyzed using the unpaired two-tailed student's t test and the log rank test. *P* values of  $< 0.05$  were considered significant. Image data were processed using SpotData Pro software (Capitalbio). Differentially expressed genes were identified using SAM package (Significance Analysis of Microarrays, version 2.1).

## Results

*miR-130a is aberrantly down-regulated in CML tissues and is inversely associated with lymph node metastasis.*

Previous microarray results showed that miR-130a is significantly down-regulated in CML. To confirm these results, quantitative real-time RT-PCR (qRT-PCR) analysis was performed in 54 coupled samples of CML cancer stem cells and corresponding normal MSCs. We found that 88.24% (45/54) of the CML cancer stem cells showed aberrant down-regulation of miR-130a compared with normal MSCs ( $1.74 \pm 0.11$  vs  $4.37 \pm 0.10$ ,  $p < 0.001$ ; **Figure 1A**).

Moreover, ROC curve analysis using miR-130a expression was used as a diagnostic marker in CML patients (**Figure 1B**). Hierarchical clustering analysis showed that miR-130a was significantly differentially expressed between CML

## Mir-130a targets RECK in CML

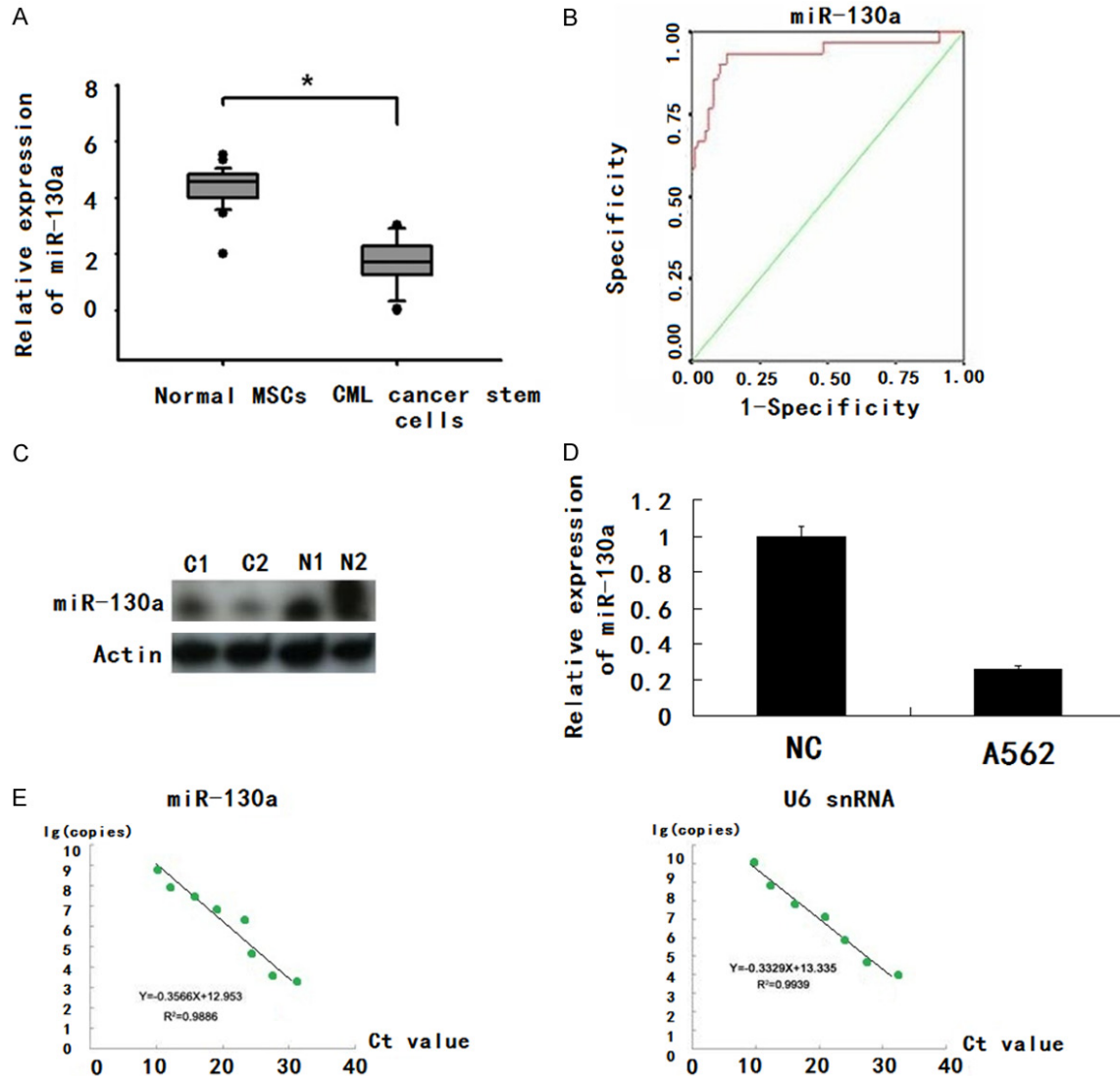
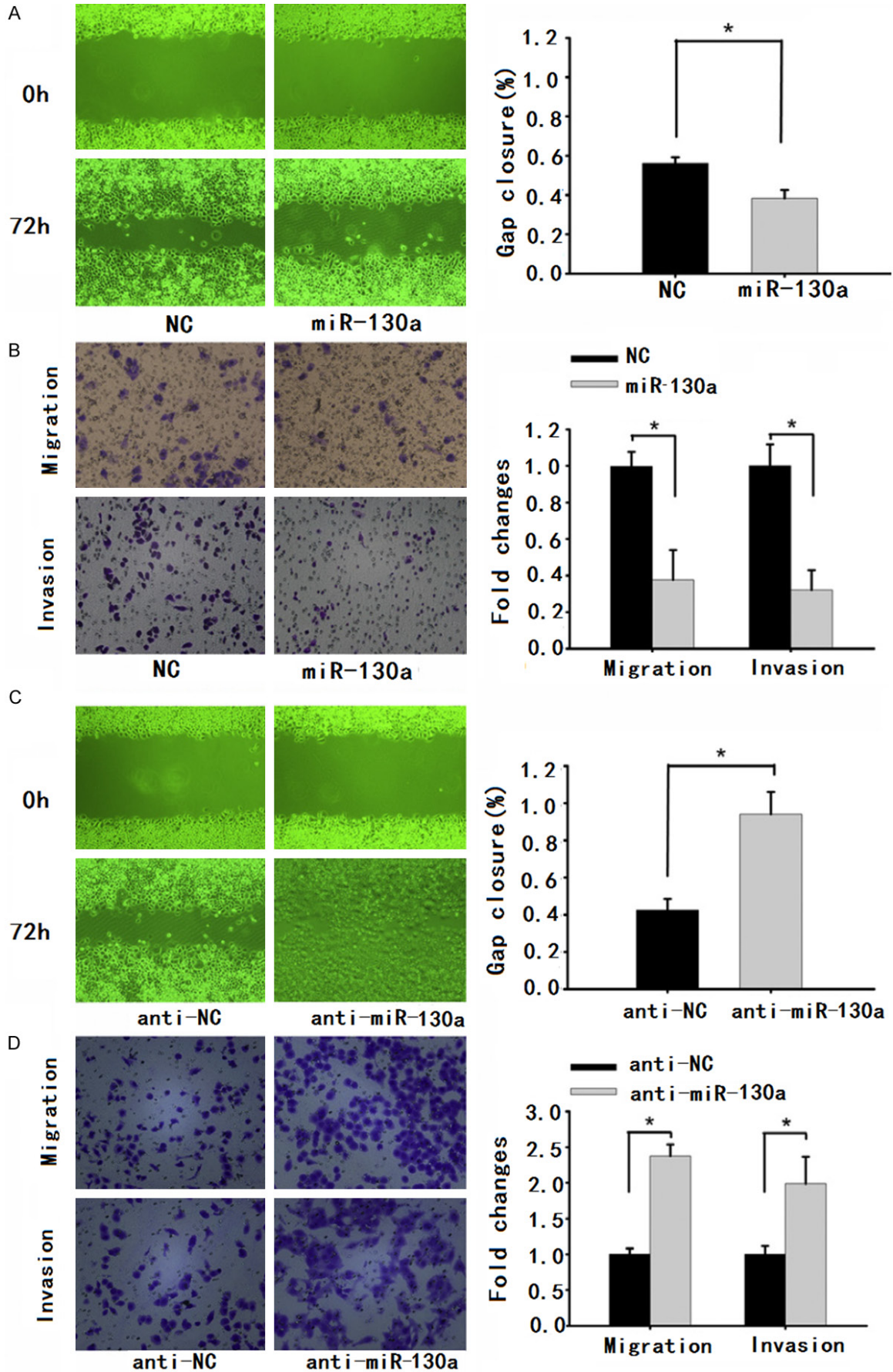


**Figure 1.** miR-130a is down-regulated in CML cancer stem cells and cell line A562. A. qRT-PCR for miR-130a in 54 matched human CML cancer stem cells and corresponding normal mesenchymal stem cells (MSCs). \* $p < 0.001$ . B. ROC curve analysis using miR-130a expression as diagnostic markers in CML patients. C. Hierarchical clustering analysis showed that miR-130a was significantly differentially expressed between CML patients and normal subjects (C-1, C-2: CML patients; N-1, N-2: normal controls). D. qRT-PCR for miR-130a in CML cell line A562 and normal control cells. \* $p < 0.05$   $n=3$ . E. Standard curve of RT-PCR was used to perform the absolute quantification analysis. The range of the reference values (copy number/ $\mu\text{g}$  total RNA) of miR-130a was  $2.7 \times 10^8 \sim 1.8 \times 10^9$ . In an absolute method, the accuracy was assured by the consistent sample loading (consistent U6 snRNA copy number). From these results, the range of ratios of miR-130a copy number to U6 snRNA copy number in normal human subject blood was  $9.29 \sim 56.78 \times 10^{-3}$ . The results that fall below the lower limit of the normal reference ratio range would be considered as a reference diagnostic criteria for CML.

patients and normal subjects (C-1, C-2: CML patients; N-1, N-2: normal controls; **Figure 1C**) (qRT-PCR for miR-130a in CML cell line A562 and normal control cell; \* $p < 0.05$ ,  $n=3$ ; **Figure 1D**). The standard curve of RT-PCR was used to perform the absolute quantification analysis. The range of the reference values (copy number/ $\mu\text{g}$  total RNA) of miR-130a was  $2.7 \times 10^8 \sim 1.8 \times 10^9$ . In an absolute method, the

accuracy was assured by the consistent sample loading (consistent U6 snRNA copy number). From these results, the range of ratios of miR-130a copy number to U6 snRNA copy number in normal human subject blood was  $9.29 \sim 56.78 \times 10^{-3}$ . The results that are below the lower limit of the normal reference ratio range would be considered as diagnostic criteria for CML (**Figure 1E**).

Mir-130a targets RECK in CML



## Mir-130a targets RECK in CML

**Figure 2.** miR-130a regulates migration and invasion *in vitro*. Wound-healing assays (A) migration and invasion assays (B) after transfection with miR-130a or NC in A562 cells. Wound-healing assays (C) migration and invasion assays (D) after transfection with anti-miR-130a or anti-NC in control cells n=3.

### *Ectopic miR-130a inhibits the migration and invasion of CML cells in A562 cells*

Based on the above results, we detected whether miR-130a can change the capacity of CML cells for migration and invasion. A562 cells were selected for restoration of miR-130a using transient gene transfection. As expected, transfection of miR-130a mimics into A562 cells resulted in a substantial increase in miR-130a expression compared with negative control (NC) transfected cells. As shown in **Figure 2A**, tumor cells with miR-130a restoration closed the scratch wounds more slowly than the control ( $38.35 \pm 0.35\%$  vs  $56.25 \pm 0.25\%$ ,  $p=0.006$ ). Moreover, the cell migration and invasion assay showed that miR-130a restoration resulted in reduced migration rate ( $2.63 \pm 0.10$ -fold,  $p=0.007$ ) and invasion rate ( $3.03 \pm 0.14$ -fold,  $p=0.005$ ) of A562 cells compared with the control (**Figure 2B**).

### *Knockdown of miR-130a promotes the migration and invasion of A562 cells*

Knockdown of miR-130a in A562 cells resulted in a significantly closer gap in the wound-healing assay ( $94 \pm 0.97\%$  vs  $42.5 \pm 0.55\%$ ,  $p=0.006$ ) and reduction of cell migration ( $2.38 \pm 0.04$ -fold,  $p=0.001$ ) and invasion ( $1.99 \pm 0.09$ -fold,  $p=0.005$ ) in transwell assays compared with anti-NC (**Figure 2C** and **2D**). These data show that miR-130a is an important participant in the regulation of migration and invasion potential of CML cells.

### *Up-regulation of miR-130a expression induces CML cells apoptosis*

To investigate the mechanism of miR-130a on CML cell growth inhibitory effects, we performed apoptosis and cell cycle analysis by flow cytometry. Our data show that approximately 10-15% of A562/miR-130a mimics transfectants exhibited morphologic features typical of apoptosis, including condensed chromatin and nuclear fragmentation by Hoechst 33342 staining and flow cytometry for DNA content. Flow cytometry indicated that the apoptotic rate was significantly increased in miR-130a

mimics transfectants compared to the control and parental cells ( $11.94 \pm 1.34\%$  vs.  $7.43 \pm 0.90\%$ ,  $6.70 \pm 0.93\%$ ,  $P < 0.01$ , **Figure 3A**, **3B** and **3D**). A562/miR-130a mimics transfectants appeared to show a higher percentage of G0/G1 phase cells ( $58.8 \pm 1.4\%$  vs.  $54.9 \pm 1.4\%$ ,  $53.5 \pm 1.7\%$ ) and a lower percentage of S phase cells ( $24.7 \pm 1.7\%$  vs.  $29.9 \pm 3.9\%$ ,  $27.7 \pm 2.5\%$ ). However, there was no significant difference in cell cycle between differently treated groups after statistical analysis ( $P > 0.05$ , **Figure 3C** and **3E**). These results indicate that over-expression of miR-130a induces apoptosis in A562 cells, which contributes to the growth inhibitory properties of miR-130a.

### *RECK is a target gene of miR-130a*

To identify how miR-130a exerts its role in CML, we searched for its putative target genes with potential pro-oncogenic functions using online search tools (e.g., MicroCosm, TargetScan, and Mirrna.org). The genes predicted by all of the bio-informatic tools were chosen as the candidate target genes of miR-130a. Among these genes, RECK, which is highly expressed in CML cells and acts as a transcriptional repressor that plays a crucial role in the signaling pathways regulating cell apoptosis [14], was identified as one potential miR-130a binding site within its 3'UTR (**Figure 4A**). We then performed luciferase reporter assays to verify a direct interaction between miR-130a and the 3'UTR of RECK. Luciferase reporters were constructed containing either a wild-type RECK 3'UTR sequence containing the miR-130a binding site (pMIR/RECK) or a mutated RECK 3'UTR (mutated CAAT to GTTA, pMIR/RECK/mut) (**Figure 4A**). The pMIR/RECK and pMIR/RECK/mut luciferase reporter constructs were transfected into HEK 293T cells, along with miR-130a or negative control mimics. The relative luciferase activity of the pMIR/RECK reporter was markedly suppressed by 45% ( $P < 0.01$ ) compared with that of pMIR/RECK/mut in a miR-130a-dependent manner (**Figure 4B**). This result strongly indicates that 3'UTR of RECK carries the direct binding sites of miR-130a. Furthermore, to determine whether miR-130a down-regulated RECK at the mRNA level or the protein level,

Mir-130a targets RECK in CML

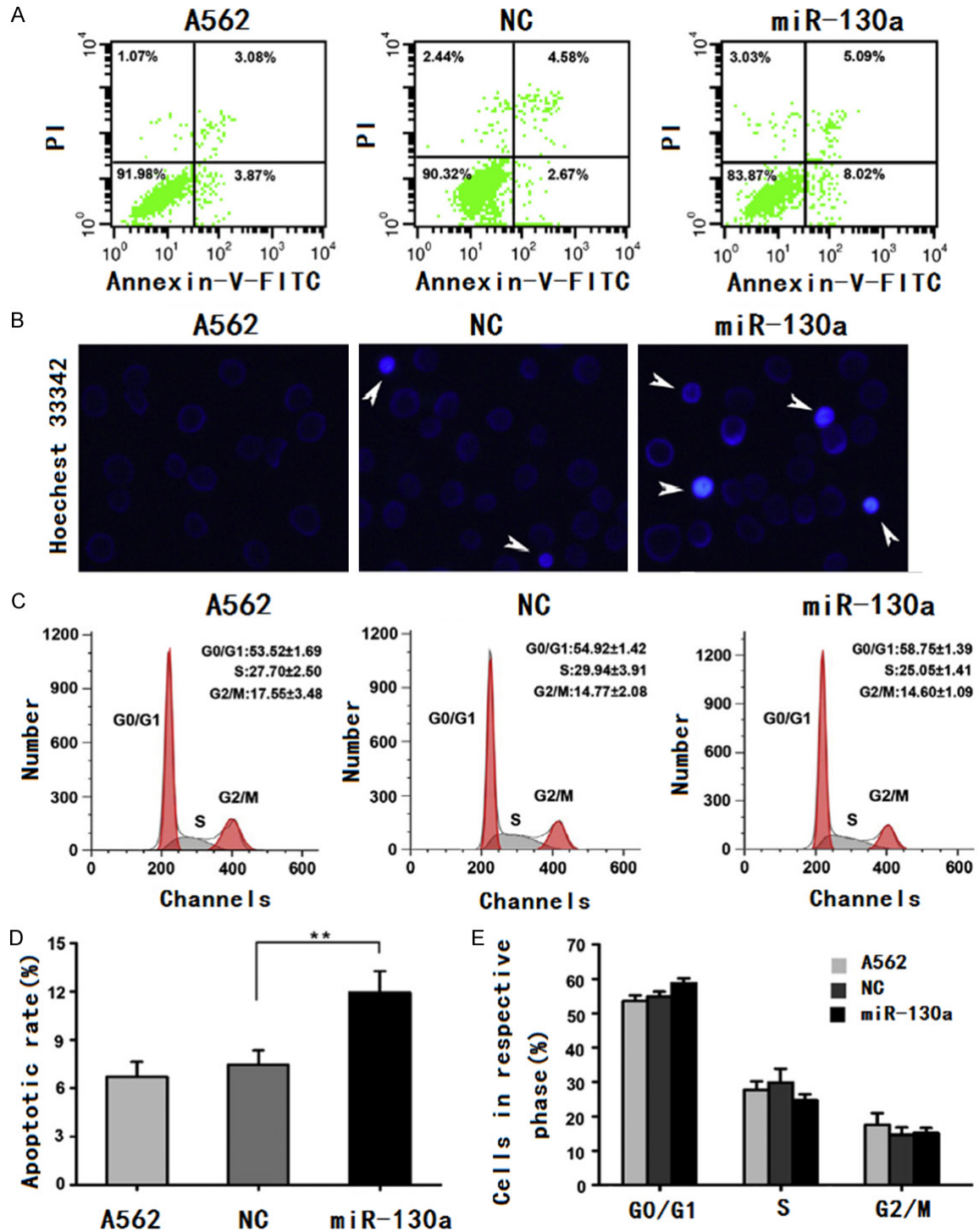


**Figure 3.** Effect of miR-130a on apoptosis and cell cycle of A562 cells. **A.** Representative histograms depicting apoptosis of A562 cells transiently transfected with 100 nM miR-130a mimics or control and parental cells. **B.** Representative histograms depicting nuclear morphology of A562 cells transiently transfected with 100 nM miR-130a mimics or control and parental cells with Hoechst 33342 (original magnification 400×). **C.** Representative histograms depicting cell cycle profiles of A562 cells transiently transfected with 100 nM miR-130a mimics or control and parental cells. **D.** Proportion of cells in various phases of the cell cycle. The results are means of three independent experiments ± S.D. **E.** The percentage of apoptotic cells of three independent experiments ± S.D. are shown (\*\* $P < 0.01$ ).

## Mir-130a targets RECK in CML

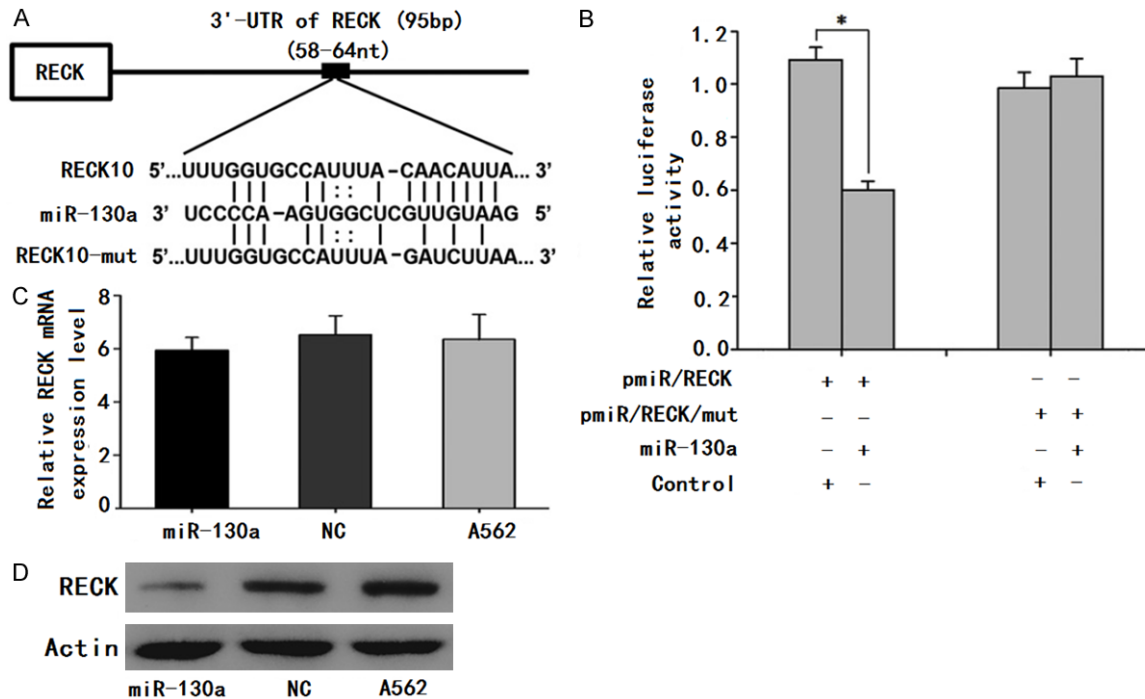


**Figure 4.** MiR-130a targets 3'UTR of RECK gene. A. Schematic graph of the putative binding sites of miR-130a in the RECK 3'UTR predicted by microRNA.org. RECK-mut indicates the RECK-3'UTR with mutation in miR-130a-binding sites. B. miR-130a mimics down-regulated luciferase activities controlled by wild-type RECK 3'UTR (\*\*P < 0.01), but did not affect luciferase activity controlled by mutant RECK 3'UTR. The results are the means of three independent experiments  $\pm$  S.D. C. RECK mRNA in A562 cells was analyzed by qRT-PCR at 48 h post-transfection with miR-130a mimics and control. D. Forty-eight hours after miR-130a mimics and control transfection on A562 cells, RECK protein level was significantly decreased in miR-130a transfected cells by Western blot.

we detected RECK expression by qRT-PCR and Western blot assays. As shown in **Figure 4D**, the RECK protein level was decreased in miR-130a mimics-transfected A562 cells compared with negative control-transfected and parental A562 cells. Nevertheless, qRT-PCR analysis of RECK showed that miR-130a had no effect on the RECK mRNA level (**Figure 4C**). These results strongly suggest that miR-130a negatively regulates RECK expression at the translational level.

### *Over-expression of miR-130a inhibits tumorigenicity and increases apoptosis in vivo*

We next examined whether over-expression of miR-130a could suppress tumor growth and induce apoptosis *in vivo*. Retrovirus-mediated A562/miR-130a and A562/miR-control stable cell lines were obtained as described in the retroviral transfection for stable cell lines section. RV-miR-130a, RV-miR-control or A562 cells were injected subcutaneously into nude mice, and tumor formation was monitored. After 35 days, the mice were euthanized, and tumor

weights were measured. Tumors grew faster in RV-miR-control and the parental cell A562 group than in the RV-miR-130a group (**Figure 5A-D**). The average weight of tumors resulting from RV-miR-130a was significantly lower than that of tumors derived from RV-miR-control or A562 cells ( $580 \pm 190$  mg vs.  $1610 \pm 570$  mg,  $1760 \pm 450$  mg;  $P < 0.01$ ). There was no significant difference in tumor volume or weight between RV-miR-control or A562 cells.

In addition, immunohistochemical analysis of Ki-67 antigen revealed that the decreased tumor growth in mice was, in part, due to lower proliferation caused by the overexpression of miR-130a. The number of Ki-67-antigen-positive cells was lower in the tumor derived from RV-miR-130a cells than that in RV-miR-control or A562 cells ( $P < 0.01$ , **Figure 5E** and **5F**). Thus, tumorigenicity was significantly reduced in RV-miR-130a cells *in vivo*. To assess whether tumor growth inhibition in RV-miR-130a was due partly to the induction of apoptosis, TUNEL assays of tumor tissues were performed. As shown in **Figure 5E** and **5G**, the

## Mir-130a targets RECK in CML

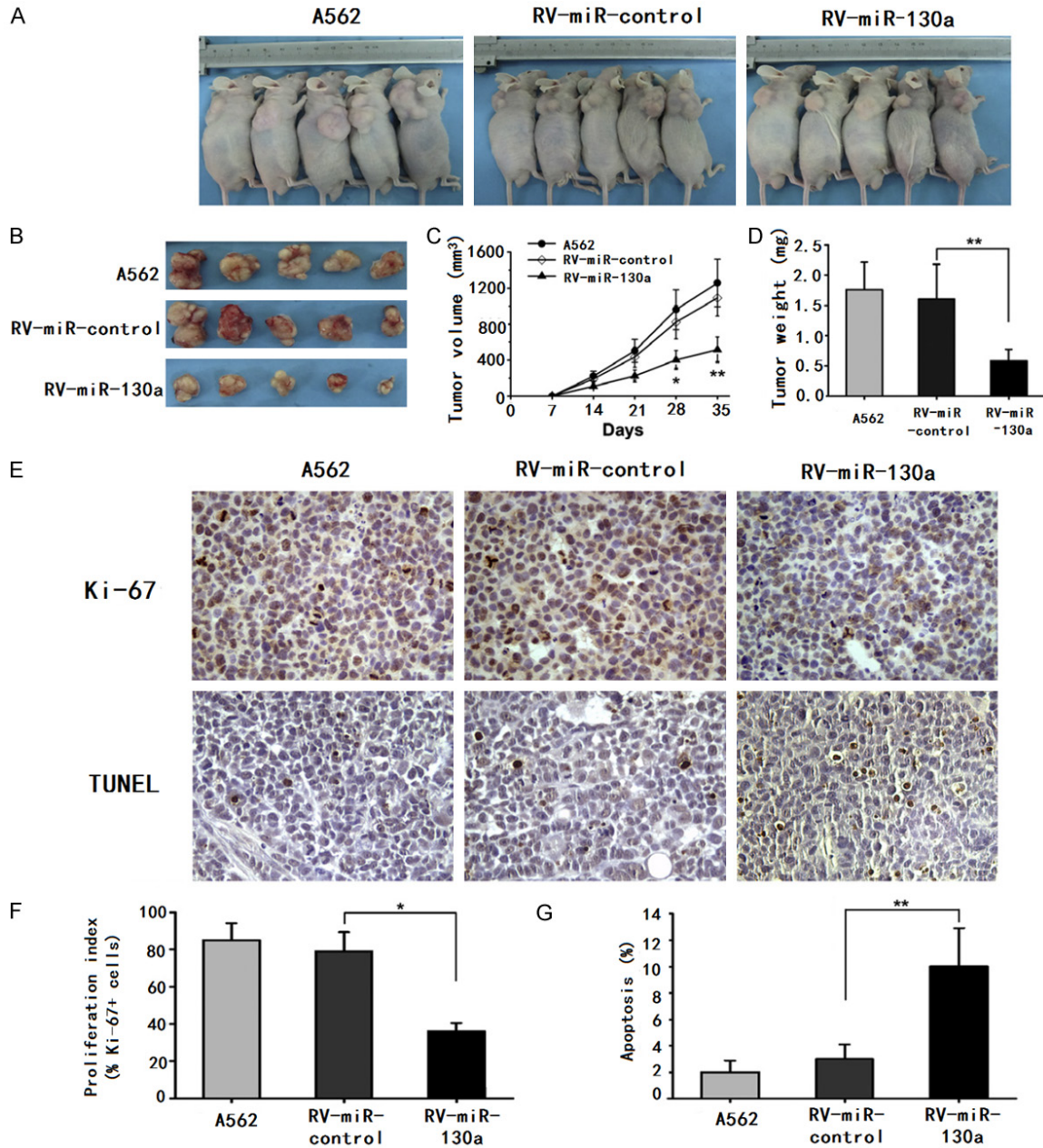


**Figure 5.** Over-expression of miR-130a inhibits tumorigenicity and increases apoptosis *in vivo*. A and B. Photographs of tumors derived from RV-miR-130a, RV-miR-control or A562 cells in nude mice. C. Growth kinetics of tumors in nude mice. Tumor diameters were measured every 7 days. (\*P < 0.05, \*\*P < 0.01). D. Average weight of tumors in nude mice. The means ± S.D. was shown (\*\*P < 0.01). E. Representative photographs of immunohistochemical analysis of Ki-67 antigen in tumors of nude mice. Representative image of TUNEL assay of tumor specimens from nude mice (original magnification, 200×). F. Comparison of proliferation index. The means ± S.D. are shown (\*P < 0.05). G. The percentage of apoptotic cells was counted. Columns, mean; bars, ± S.D. (\*\*P < 0.01).

RVmiR-130a cells showed more tumor cell positive staining and a significantly higher apoptotic index than the A562/vector or A562 cells ( $P < 0.01$ ). These results suggest that miR-130a inhibition of tumorigenicity is attributed to decreased proliferation and increased apoptosis *in vivo*.

*miR-130a inhibits the protein expression of RECK by directly targeting 3'-UTR of RECK*

TargetScan and miRanda algorithms were used to predict the mRNA targets of miR-130a and identify effectors of miR-130a. Numerous possible candidates were identified through this

## Mir-130a targets RECK in CML

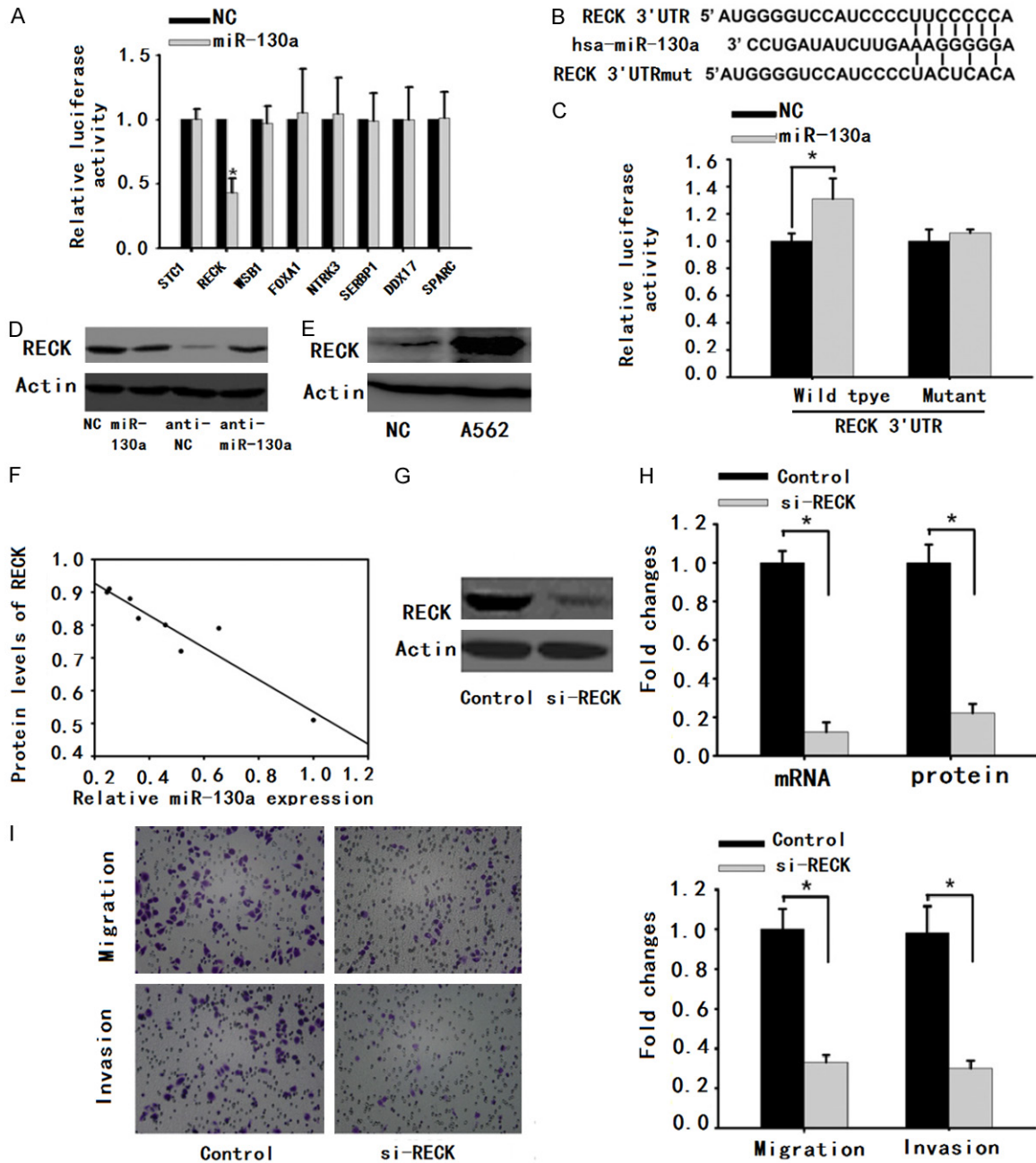


**Figure 6.** miR-130a inhibits the protein expression of RECK and knockdown of RECK inhibits cellular migration and invasion in A562 cells. **A.** Luciferase activity in A562 cells transfected with miR-130a or NC after transfection of the indicated 3'-UTR driven reporter constructs n=3. **B.** The wild type and mutant complementary sequences of the RECK mRNA 3'-UTR are shown with the miR-130a sequence. **C.** Luciferase activity in HELF cells transfected with anti-miR-130a or anti-NC n=3. **D.** Immunoblots for RECK in the A562 cells transfected with miR-130a or NC and in the HELF cells transfected with anti-miR-130a or anti-NC n=3. **E.** Immunoblots for RECK in the CML cell lines A562 and HELF cells. **F.** Correlation between miR-130a and RECK protein levels via measuring grey levels of immunoblots in CML cell lines and HELF cells.  $R=-0.949$ ,  $p < 0.001$  by Spearman correlation. **G, H.** Immunoblots and qRT-PCR for RECK in the A562 cells transfected with si-RECK or control. **I.** Migration and invasion assays in A562 cells with si-RECK or control n=3.

process. From these candidates, we chose those that were over-expressed in cancers and metastasis-associated genes, including STC1, RECK, WSB1, FOXA1, NTRK3, SERBP1, DDX17

and SPARC. The 3'-UTRs of these genes were cloned into the pMIR-report plasmid. The luciferase assay showed that the activity of the reporter containing the 3'-UTR of the RECK

## Mir-130a targets RECK in CML

gene was decreased by 56.9% ( $p=0.002$ ) following treatment with miR-130a mimics, whereas the reporter activity containing the 3'-UTRs of the other genes were not obviously altered in 293T cells (**Figure 6A** and **6B**). In contrast, when miR-130a inhibitors were transfected, wild-type reporter activity was increased in 293T cells compared with the control ( $1.31 \pm 0.08$ -fold,  $p=0.008$ ), but mutant reporter activity did not change (**Figure 6C**). Next, we investigated whether miR-130a modulated the protein expression of RECK using immunoblots. We observed that RECK protein levels were decreased when miR-130a was restored in A562 cells. A reverse result was observed when miR-130a was knocked down in HELF cells (**Figure 6D**).

*The expression of miR-130a is inversely correlated with the expression of RECK protein*

To further confirm RECK is a target of miR-130a, we measured RECK protein levels in A562 and control cells (**Figure 6E**) and investigated the relationship between expression levels of miR-130a and protein levels of RECK. A significant inverse correlation was observed between the expression of miR-130a and RECK protein in these cell lines ( $R=-0.949$ ,  $p < 0.001$ , **Figure 6F**).

*Knockdown of RECK inhibits cellular migration and invasion in vitro*

To confirm the effects of RECK on the migration and invasion of A562 cells, RECK expression was knocked down by a RECK siRNA. qRT-PCR and immunoblot analyses showed that the si-RECK transfection of A562 cells effectively inhibited approximately 87.6% of mRNA expression and 77.9% of protein expression of RECK, when compared to control groups (**Figure 6G**, **6H**). Consequently, wound-healing and transwell assays examining migration and invasion were performed. Decreased migration ( $3.40 \pm 0.15$ -fold,  $p=0.002$ ) and invasion ( $3.28 \pm 0.20$ -fold,  $p=0.003$ ) were observed in A562 cells transfected with si-RECK compared to the controls (**Figure 6I**). These data suggest that knockdown of RECK suppresses migration and invasion in A562 cells and RECK is an effective target gene of miR-130a

### Discussion

In this study, we demonstrated the inhibitory effects of miR-130a on tumor metastasis at the clinical, animal experimental, cellular and

molecular levels. We found that miR-130a expression was down-regulated in CML and involved in lymph node metastasis. Restoration of miR-130a in A562 cells significantly impaired cellular migration and invasion *in vitro* and *in vivo*. In contrast, knockdown of miR-130a in A562 cells reversed the effects. Screened from eight putative genes based on bioinformatic algorithms, RECK was found to be a target gene of miR-130a. The tumor metastasis-associated effects of RECK were consistent with the functions of miR-130a on the phenotypes in A562 cells [15].

Recent studies have clearly demonstrated the important roles of miRNAs in CML as well as other malignant diseases. Although miRNA signatures for CML have been established, elucidation of the roles of dysregulated miRNAs in CML carcinogenesis remains elusive. In this study, we provide the detailed mechanistic experimental evidence of miR-130a in CML by suppressing the expression of RECK. MiR-130a, located on 14q32.31, has been reported to regulate fibrinogen production by lowering fibrinogen Bb mRNA levels in blood [1]. miR-130a was found to be significantly under-expressed in pancreatic ductal adenocarcinoma compared with normal controls and/or chronic pancreatitis by miRNA microarrays [16]. Reports also identified down-regulated expression of miR-130a in hepatoma Huh7 cells compared with normal hepatocytes by microarray analysis [17]. Early evidence found miR-130a was associated with CML depth of invasion and peritoneal dissemination [18]. However, all of these findings are based on miRNA microarrays and need to be confirmed by quantitative real-time PCR. Recent reports showed that the expression of miR-409 was reduced in CML cell lines with CpG-rich methylation and that its expression could be restored by treatment with demethylated drugs [19]. Some research has indicated that miR-130a suppressed CML cell invasion and metastasis by directly targeting RDX and suggested that it acted as a new anti-metastatic miRNA in CML [20].

In this study, we identify miR-130a as a candidate tumor suppressor in CML. We found down-regulation of miR-130a expression in both CML cancer stem cells and cell lines. Restoration of miR-130a in A562 cells significantly reduced proliferation and induced apoptosis both *in vitro* and *in vivo*. These results suggest that miR-130a may have tumor suppressive func-

## Mir-130a targets RECK in CML

tions in human CML. It seems that as a novel tumor suppressor, miR-130a has multiple functions on CML tumor cells [21-24]. MiR-130a that bound with incomplete complementarity to RECK mRNA, occurring within the 3'UTR of the transcript, was assumed to exclusively direct translational inhibition of RECK mRNA but not affect overall mRNA stability. RECK belongs to a family of plant homeodomain (PHD) containing proteins that play a role in regulating transcription via chromatin remodeling [25, 26]. Convincing evidence has also shown that RECK is over-expressed in many types of malignant tumors including colon cancer and gastric cancer [14]. We previously identified that RECK was over-expressed in CML cell lines and acted as an oncogene in CML. Direct binding of RECK to the promoter region of caspase-3 led to the down-regulation of caspase-3 protein levels. Knockdown of RECK induced apoptosis and resulted in the accumulation of caspase-3 and activation of its substrates [14]. We found that RECK was up-regulated in CML tissues compared with non-tumor tissues and associated with CML clinicopathologic parameters (unpublished data). RECK function is also required for cell proliferation. Depletion of RECK function by RNAi causes loss of cell proliferation in normal control cells [27]. Furthermore, several results from our study indicate that RECK is a direct target gene of miR-130a in CML. First, over-expression of miR-130a remarkably decreases the activity of a luciferase reporter containing the 3'UTR of RECK, while mutation of the "seed region" sites in the 3'UTR of RECK abolishes the miR-130a regulation effect. Second, human CML tissues express significantly lower levels of miR-130a than non-tumor tissues, and concomitantly, CML tissues contain significantly higher levels of RECK protein than non-tumor tissues. Third, over-expression of miR-130a down-regulates RECK at the protein level. The biological relevance of RECK as a miR-130a target is supported by demonstrating that RECK silencing can also reduce cell proliferation and induce apoptosis while RECK over-expressing can partially reverse the effects of miR-130a.

One of the mechanisms of miR-130a involved in the increase of cell apoptosis is its down-regulation of RECK and activation of caspase-3. However, we cannot rule out other important targets and pathways as a single miRNA can target multiple mRNAs. Further study is required to identify other targets and pathways of miR-130a. In addition, the detailed mecha-

nisms for reduced miR-130a expression in CML remains to be further investigated.

In conclusion, our data suggest that miR-130a may act as a novel tumor suppressor miRNA in CML, and down-regulation of miR-130a may be required for CML carcinogenesis, at least in part, through the up-regulation of the RECK oncogene. By identifying the mechanism and function of miR-130a as a tumor suppressor, it may eventually be possible to develop miR-130a as a novel therapeutic strategy in CML treatment.

### Disclosure of conflict of interest

None.

**Address correspondence to:** Tienan Yi, Department of Oncology, Xiangyang Central Hospital, Hubei University of Arts and Science, Jinzhou Road 136#, Xiangyang 441053, China. E-mail: 25036256@qq.com; Weiming Li, Department of Hematology, Union Hospital, Tongji Medical College, Huazhong University of Science and Technology, 1277# Jiefang Avenue, Wuhan 430022, China. E-mail: liweimingvip@163.com

### References

- [1] Cai J, Wu G, Tan X, Han Y, Chen C, Li C, Wang N, Zou X, Chen X, Zhou F, He D, Zhou L, Jose PA and Zeng C. Transferred BCR/ABL DNA from K562 extracellular vesicles causes chronic myeloid leukemia in immunodeficient mice. *PLoS One* 2014; 9: e105200.
- [2] Joshi D, Chandrakala S, Korgaonkar S, Ghosh K and Vundinti BR. Down-regulation of miR-199b associated with imatinib drug resistance in 9q34.1 deleted BCR/ABL positive CML patients. *Gene* 2014; 542: 109-112.
- [3] Nishioka C, Ikezoe T, Yang J, Nobumoto A, Tsuda M and Yokoyama A. Downregulation of miR-217 correlates with resistance of Ph(+) leukemia cells to ABL tyrosine kinase inhibitors. *Cancer Sci* 2014; 105: 297-307.
- [4] Karimiani EG, Marriage F, Merritt AJ, Burthem J, Byers RJ and Day PJ. Single-cell analysis of K562 cells: an imatinib-resistant subpopulation is adherent and has upregulated expression of BCR-ABL mRNA and protein. *Exp Hematol* 2014; 42: 183-191, e185.
- [5] Shibuta T, Honda E, Shiotsu H, Tanaka Y, Vellasamy S, Shiratsuchi M and Umemura T. Imatinib induces demethylation of miR-203 gene: an epigenetic mechanism of anti-tumor effect of imatinib. *Leuk Res* 2013; 37: 1278-1286.
- [6] Hamerschlak N, Souza CD, Cornacchioni AL, Pasquini R, Tabak D, Spector N and Steagall M.

## Mir-130a targets RECK in CML

- Patients' perceptions about diagnosis and treatment of chronic myeloid leukemia: a cross-sectional study among Brazilian patients. *Sao Paulo Med J* 2015; 133: 471-9.
- [7] Eichelser C, Stuckrath I, Muller V, Milde-Langosch K, Wikman H, Pantel K and Schwarzenbach H. Increased serum levels of circulating exosomal microRNA-373 in receptor-negative breast cancer patients. *Oncotarget* 2014; 5: 9650-9663.
- [8] Zhang M, Luo W, Huang B, Liu Z, Sun L, Zhang Q, Qiu X, Xu K and Wang E. Overexpression of JAM-A in non-small cell lung cancer correlates with tumor progression. *PLoS One* 2013; 8: e79173.
- [9] Xishan Z, Xianjun L, Ziyang L, Guangxin C and Gang L. The malignancy suppression role of miR-23a by targeting the BCR/ABL oncogene in chronic myeloid leukemia. *Cancer Gene Ther* 2014; 21: 397-404.
- [10] Zhang J, Wang P, Zhu J, Wang W, Yin J, Zhang C, Chen Z, Sun L, Wan Y, Wang X, Chen G and Liu Y. SPARC expression is negatively correlated with clinicopathological factors of gastric cancer and inhibits malignancy of gastric cancer cells. *Oncol Rep* 2014; 31: 2312-2320.
- [11] Bubnovskaya I, Kovelskaya A, Gumenyuk L, Ganusevich I, Mamontova L, Mikhailenko V, Osinsky D, Merentsev S and Osinsky S. Disseminated tumor cells in bone marrow of gastric cancer patients: correlation with tumor hypoxia and clinical relevance. *J Oncol* 2014; 2014: 582140.
- [12] Chen X, Shi X, Zhao C, Li X, Lan X, Liu S, Huang H, Liu N, Liao S, Zang D, Song W, Liu Q, Carter BZ, Dou QP, Wang X and Liu J. Anti-rheumatic agent auranofin induced apoptosis in chronic myeloid leukemia cells resistant to imatinib through both Bcr/Abl-dependent and -independent mechanisms. *Oncotarget* 2014; 5: 9118-9132.
- [13] Shibazaki M, Sumi M, Takeda W, Kirihara T, Kirihara T, Sato K, Ueki T, Hiroshima Y, Ueno M, Ichikawa N, Mori Y and Kobayashi H. [Therapy-related chronic myelogenous leukemia following RFM therapy in a patient with follicular lymphoma]. *Rinsho Ketsueki* 2014; 55: 970-974.
- [14] Hussein K, Busche G, Muth M, Gohring G, Kreipe H and Bock O. Expression of myelopoiesis-associated microRNA in bone marrow cells of atypical chronic myeloid leukaemia and chronic myelomonocytic leukaemia. *Ann Hematol* 2011; 90: 307-313.
- [15] Wei S, Wang Y, Chai Q, Fang Q, Zhang Y, Lu Y and Wang J. Over-expression of heme oxygenase-1 in peripheral blood predicts the progression and relapse risk of chronic myeloid leukemia. *Chin Med J (Engl)* 2014; 127: 2795-2801.
- [16] Rondanin R, Simoni D, Romagnoli R, Baruchello R, Marchetti P, Costantini C, Fochi S, Padroni G, Grimaudo S, Pipitone RM, Meli M and Tolomeo M. Inhibition of activated STAT5 in Bcr/Abl expressing leukemia cells with new pimozone derivatives. *Bioorg Med Chem Lett* 2014; 24: 4568-4574.
- [17] Li Y, Yuan Y, Tao K, Wang X, Xiao Q, Huang Z, Zhong L, Cao W, Wen J and Feng W. Inhibition of BCR/ABL protein expression by miR-203 sensitizes for imatinib mesylate. *PLoS One* 2013; 8: e61858.
- [18] Li Y, Wang H, Tao K, Xiao Q, Huang Z, Zhong L, Cao W, Wen J and Feng W. miR-29b suppresses CML cell proliferation and induces apoptosis via regulation of BCR/ABL1 protein. *Exp Cell Res* 2013; 319: 1094-1101.
- [19] Verma M, Karimiani EG, Byers RJ, Rehman S, Westerhoff HV and Day PJ. Mathematical modelling of miRNA mediated BCR.ABL protein regulation in chronic myeloid leukaemia vis-a-vis therapeutic strategies. *Integr Biol (Camb)* 2013; 5: 543-554.
- [20] Xishan Z, Xu Z, Lawei Y and Gang L. Hemangioblastic characteristics of cancer stem cells in chronic myeloid leukemia. *Clin Lab* 2012; 58: 607-613.
- [21] Liu Y, Song Y, Ma W, Zheng W and Yin H. Decreased microRNA-30a levels are associated with enhanced ABL1 and BCR-ABL1 expression in chronic myeloid leukemia. *Leuk Res* 2013; 37: 349-356.
- [22] Lopotova T, Zackova M, Klamova H and Moravcova J. MicroRNA-451 in chronic myeloid leukemia: miR-451-BCR-ABL regulatory loop? *Leuk Res* 2011; 35: 974-977.
- [23] Xu C, Fu H, Gao L, Wang L, Wang W, Li J, Li Y, Dou L, Gao X, Luo X, Jing Y, Chim CS, Zheng X and Yu L. BCR-ABL/GATA1/miR-138 mini circuitry contributes to the leukemogenesis of chronic myeloid leukemia. *Oncogene* 2014; 33: 44-54.
- [24] Fei J, Li Y, Zhu X and Luo X. miR-181a post-transcriptionally downregulates oncogenic RalA and contributes to growth inhibition and apoptosis in chronic myelogenous leukemia (CML). *PLoS One* 2012; 7: e32834.
- [25] Pellicano F, Sinclair A and Holyoake TL. In search of CML stem cells' deadly weakness. *Curr Hematol Malig Rep* 2011; 6: 82-87.
- [26] Perrotti D and Harb JG. BCR-ABL1 kinase-dependent alteration of mRNA metabolism: potential alternatives for therapeutic intervention. *Leuk Lymphoma* 2011; 52 Suppl 1: 30-44.
- [27] Eiring AM, Harb JG, Neviani P, Garton C, Oaks JJ, Spizzo R, Liu S, Schwind S, Santhanam R, Hickey CJ, Becker H, Chandler JC, Andino R, Cortes J, Hokland P, Huettner CS, Bhatia R, Roy DC, Liebhaber SA, Caligiuri MA, Marcucci G, Garzon R, Croce CM, Calin GA and Perrotti D. miR-328 functions as an RNA decoy to modulate hnRNP E2 regulation of mRNA translation in leukemic blasts. *Cell* 2010; 140: 652-665.